Temperature-Dependent Optoelectronic Characteristics of p- SnO_2/n-Si Heterojunction Structures

Adeeb Y. Bahlool

Department of Physics, College of Education, University of Misan, Amara, IRAQ

Abstract
In this work, n-type tin oxide thin films were grown on n-type silicon substrates to fabricate heterojunctions. The electrical measurements on the prepared samples were performed at different substrate and annealing temperatures. The results of these measurements showed good uniformity of these films throughout the current-voltage characteristics in both forward and reverse bias conditions at different annealing temperatures. They showed that the I-V characteristics were highly improved by thermal annealing. The reflectivity and internal quantum efficiency of the p-SnO_2/n-Si were measured as functions of the incident light wavelength. As well, the short-circuit current density and open-circuit voltage were measured as functions of the incident light intensity.

Keywords: Nanostructures; Tin dioxide; Spectroscopic characteristics; Magnetron sputtering
Received: 19 October 2023; **Revised:** 09 December; **Accepted:** 16 December; **Published:** 1 January 2024

1. Introduction

Metallic oxide semiconductors have attracted an intense interest in optoelectronic applications during the last two decades. Among them, tin oxide (SnO_2) was the subject of too many research works due to its characteristic features, especially the variation of band gap within 3.6-4.2 eV [1]. This variation is mainly determined by the preparation method and the type of substrate [2]. Controlling the deposition conditions of SnO_2 films is an important step in controlling their electrical properties, facilitating the device design [3]. Apart from the optical properties, it is of crucial importance to understand the charge transport processes in SnO_2 [4]. In this regard, the overall temperature behavior of the electrical conductivity can reveal the underlying charge transport mechanisms in this material [5]. The electron tunneling from the silicon conduction band into SnO_2 conduction band occurs at the participation of traps in the depletion region [6].

In this work, polycrystalline tin oxide (SnO_2) thin films were prepared to form heterojunctions on n-type silicon substrates and study their electrical characteristics as functions of the temperature and illumination.

For deep understanding of the conductivity behavior in the studied samples, it should be considered as a logarithmic derivation which is given by [7]:

$$W(T) = \left(\frac{T}{\sigma}\right)\frac{d\sigma}{dT} \quad (1)$$

where $W(T)$ can be used to determine the metallic and insulating behaviors of conductivity

When the slope of plot between $\ln[W(T)]$ and $\ln T$ is negative, then the sample is considered as insulator, whereas the positive slope of the $W(T)$ plot indicates that the sample is considered as metal. On the other hand, in more detail, the decrease of $W(T)$ towards zero with decreasing temperature identifies the sample as a real metal, while the temperature-independent behavior of $W(T)$ indicates that the sample is weakly insulating [8].

In polycrystalline materials, a high density of defects is expected at the grain boundaries, which are often charged with majority carriers [9]. The charged states at the grain boundaries create depleted regions and potential barriers, which provide resistance to the passage of carriers [10]. According to the grain boundaries model [11], an increase in the crystallite size (L) causes a decrease in the grain boundaries scattering and this leads to a decrease in the surface trap density (N_t).

2. Experimental Part

The substrate used was (111) n-type single crystal silicon, each of 1×1 cm^2 area with a resistivity of (1.5-4) Ω.cm. The silicon substrates were etched with CP4 solution consisting of (HNO_3, CH_3COOH, HF) of ratios (3:3:5) to

remove oxides. They were then cleaned by alcohol and ultrasonic machine (Cerry PUL 125 device) for 15 minutes then they were cleaned by water and ultrasonic waves for another 15 minutes.

High purity of tin (Sn) thin film was deposited on silicon substrate using thermal evaporation technique at room temperature under vacuum pressure of 10^{-6} torr. Tin oxide (SnO_2) film was obtained with aid of rapid thermal oxidation system with halogen lamp as oxidation source. The oxidation condition used to form SnO_2 film was 600°C/90 s. The silicon sample used it as substrate for TCO's/Si hetero-junction. Ohmic contacts were fabricated by evaporating 99.999 purity aluminum wires for back contact and 99.999 pure gold were used as front contact using Edwards coating system. The reflectance of the fabricated p-SnO_2/n-Si structure was measured using spectrophotometer type SP-H 1011.

3. Results and Discussion

Figure (2) shows ln[$W(T)$] vs. ln$T$ for the samples. The temperature-dependent $W(T)$ studies were carried out in the range of 60-200K for the samples at different deposition temperatures (T_d) as shown in Fig. (1). Here, therefore, the investigated samples exhibit metallic-like and weakly insulating behavior for T<100K and T>100 K, respectively.

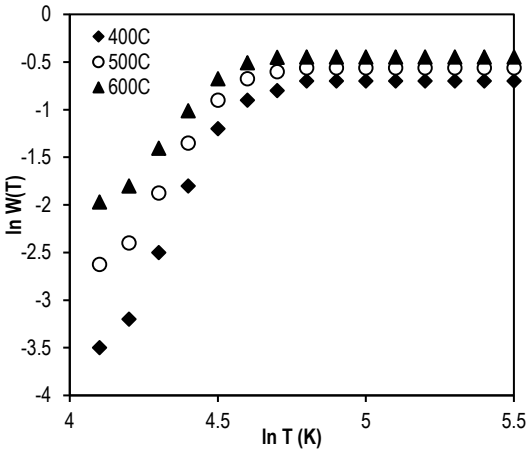

Fig. (1) Plot of ln[$W(T)$] vs. ln$T$

The plot of ln(σT)$^{1/2}$ vs. $10^3/T$ for the samples with varying deposition temperature is shown in Fig. (2). The conductivity increases rapidly with increasing temperature from 100 to 200 K, and increases slowly below 100 K. The data show the presence of two different conduction mechanisms. One is the thermoionic emission through the grain boundaries, which has activation-type temperature dependence due to the carrier activation in the grain boundaries in the temperature range above 100 K, and the other is the tunneling below 100 K, in which the conductivity may be considered to be temperature independent. We believe that this residual temperature dependence of conductivity is due to the tunneling effect. It is well known that, unlike thermionic emission, the tunneling effect is independent of temperature [12,13]. In the case of tunneling carriers can overcome the depletion region by tunneling. If tunneling takes place between the top of the barrier and the Fermi level, the thermoionic emission occurs. In this case, when the barrier height is small, carriers can surmount the barrier [14,15].

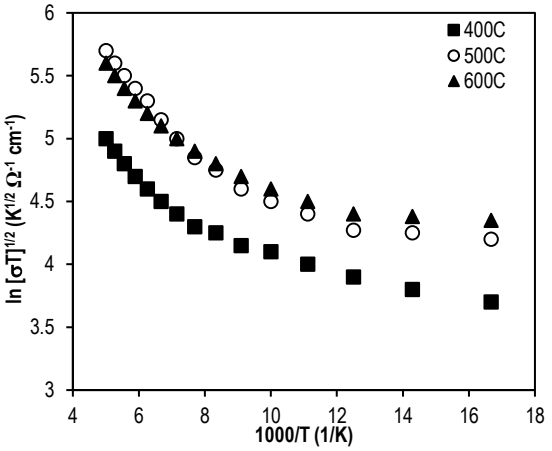

Fig. (2) Temperature dependence of the conductivity plotted as ln(σT)$^{1/2}$ vs. 1000/T

As previously mentioned, the conductivity of our samples has an activated character, including two intervals with different slopes as can be observed from Fig. (2). This situation is consistent with the behavior of W given in Fig. (1). When Fig. (1) is considered, one can expect that the high-temperature slope (T>100 K) is connected to the thermoionic emission for the samples by the following equation [17]:

$$\sigma_{TE} = \left(\frac{Le^2 n v_c}{kT}\right) e^{-\frac{E_b}{kT}} \qquad (2)$$

where E_b is the barrier height

The electrical conductivity in the tunneling regime is given as [18]:

$$\sigma_{TN} = \left(\frac{Le^2\psi}{h^2 l_2}\right) exp\left(-\frac{4\pi l_2 \psi}{h}\right) \qquad (3)$$

where

$\psi = \sqrt{2m^* E_b}$ and $l_2 = \sqrt{\frac{\varepsilon\varepsilon_0 E_b}{e^2 N_d}}$, l_2 is the depletion layer width, h is the Planck's constant, ε_0 is the dielectric constant of vacuum, ε (=11.65) is the static dielectric constant, and N_d is the donor concentration

The values of l_2 are calculated by fitting Eq. (3) to the low-temperature range shown in Fig. (2) and then the values of N_d are obtained. One can expect that the width of l_2 decreases with the increase in N_d, while the tunneling probability increases. As a consequence, the conductivity increases as the width of l_2 decreases. However, we should consider a combined effect of N_d and l_2 on the conductivity of the investigated films as explained before. Figure (3) shows the variation of depletion layer width with the doping concentration at different barrier height energies (E_b).

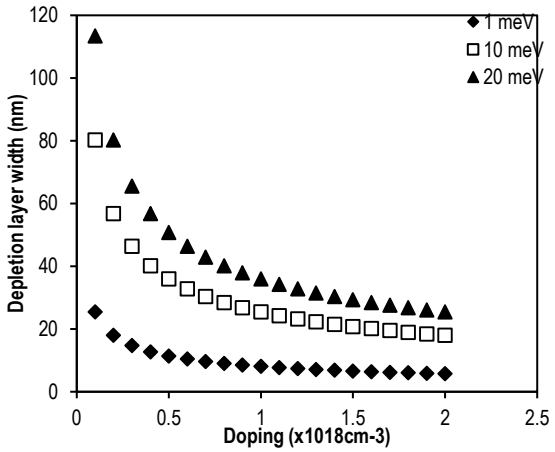

Fig. (3) Variation of depletion layer width (l_2) vs. doping concentration (N_d) at different barrier height energies (E_b)

The investigated films exhibit this expected behavior. The value of N_t of the films was found to decrease with the increase in the deposition temperature. Trapping states are capable of trapping free carriers and, as a consequence, more free carriers become immobilized as the number of trapping states increase. There are two cases: either the depletion layer (l_2) extends throughout the crystallite or only a part of the crystallite is depleted of carriers. In the latter case, the depletion layer width is smaller than the crystallite size (l_2<L) and the N_t is given as [19]:

$$N_t = \frac{\sqrt{8\varepsilon\varepsilon_0 N_d E_b}}{e} \qquad (4)$$

The SnO_2 films in this study satisfy the condition l_2<L. Utilizing Eq. (4), we can now calculate the values of N_t. The obtained N_t values agree well with the values of the surface state density for various polycrystalline systems [20,21].

The I-V characteristics of the SnO_2/Si structure for a thickness of 500 nm are shown in Fig. (4). The dark forward I-V characteristic for the p-SnO_2/n-Si structure were measured in the annealing temperature range 25-150°C, the SnO_2 thickness was 500 nm. The independence of the slope of the forward branches of the I-V characteristics on the temperature is their peculiarity. Such behavior of the forward current is characteristic for the case of tunnel processes.

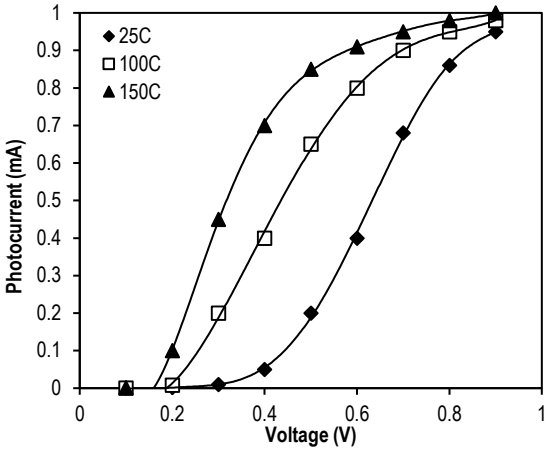

Fig. (4) The forward I-V characteristics of the SnO_2/Si structure at different annealing temperature

The doping level of n-type Si ($10^{15}cm^{-3}$) is too small for direct tunneling through the barrier, and the electron tunneling from the silicon conduction band into SnO_2 conduction band occurs at the participation of traps in the depletion region [22]. Figure (6) shows the reverse I-V characteristics of the p-SnO_2/n-Si structure at different annealing temperature.

For voltage less than 0.65 V, the reverse current is proportional to the voltage, but at voltage greater than 0.65 V, a sharp rise of current due to tunnel transition of electron from the conduction band of SnO_2 into the conduction band of Si is noticed. The reverse current is determined by the transport of the minority carries from the Si valance band to the SnO_2 conduction band for the small indirect bias up to 0.65 V. For large values of reverse voltage, the voltage drops due to the semiconductor and insulation film characteristics.

The photoelectric properties have been investigated at the illumination of the structures through the wide gap semiconductor (SnO_2). The short circuit current density depends on illumination intensity. The current starts increasing at λ>0.5μm and the maximum current obtained at wavelength equal to 0.95μm.

4. Conclusion

The results obtained in this work showed that the fabricated structures exhibit good current-voltage characteristics in both

forward and reverse bias conditions at different substrate and annealing temperatures. The electrical I-V characteristics were highly improved by thermal annealing. The optoelectronic characteristics of the fabricated structures can be optimized to employ them in solar cell applications.

References

[1] A. Ranjgar et al., "Characterization and Optical Absorption Properties of Plasmonic Nanostructured Thin Films", Armenian J. Phys., 6(4) (2013) 198-203.

[2] O.A. Hamadi, "Characteristics of CdO-Si heterostructure produced by plasma-induced bonding technique," Proc. IMechE Part L: J. Mater. Design and Applications, 222, 2008, 65–71.

[3] A. Tabata et al., "Optical properties and structure of SiO_2 films prepared by ion-beam sputtering", Thin Solid Films, 289 (1996) 84-89.

[4] A.K. Yousif and O.A. Hamadi, "Plasma-induced etching of silicon surfaces," Bulg. J. Phys., 35(3) (2008) 191–197.

[5] A.M. Al-Dhafiri, "High-Quality Plasma-Induced Crystallization of Amorphous Silicon Structures", Iraqi J. Appl. Phys., 5(1) (2009) 35-39.

[6] Hammadi OA. Effects of Extraction Parameters on Particle Size of Titanium Dioxide Nanopowders Prepared by Physical Vapor Deposition Technique, Plasmonics, 15 (2020) 1747-1754.

[7] A.T.S. Yee, "Synthesis of Silicon Nanowires by Selective Etching Process", Iraqi J. Appl. Phys., 4(3) (2008) 15-17.

[8] Bang SB, Chung TH, Kim Y, Kang MS, Kim JK, "Effects of the oxygen fraction and substrate bias power on the electrical and optical properties of silicon oxide films by plasma enhanced chemical vapour deposition using TMOS/O_2 gas", J. Phys. D: Appl. Phys., 37 (2004) 1679-1684.

[9] E.S.M. Goh, T.P. Chen, C.Q. Sun and Y.C. Liu, "Thickness effect on the band gap and optical properties of germanium thin films", J. Appl. Phys., 107 (2010) 024305.

[10] O.A. Hammadi, "Characteristics of Heat-Annealed Silicon Homojunction Infrared Photodetector Fabricated by Plasma-Assisted Technique", Phot. Sens., 6(4) (2016) 345-350.

[11] H. Jung, W.H. Kim, I.K. Oh, C.W. Lee, C. Lansalot-Matras, S.J. Lee, J.M. Myoung, H.B. Ram Lee and H. Kim, "Growth characteristics and electrical properties of SiO_2 thin films prepared using plasma-enhanced atomic layer deposition and chemical vapor deposition with an aminosilane precursor", J. Mater. Sci., 51(11) (2016) 5082-5091.

[12] O.A. Hammadi, "Characterization of SiC/Si Heterojunction Fabricated by Plasma-Induced Growth of Nanostructured Silicon Carbide Layer on Silicon Surface", Iraqi J. Appl. Phys., 12(2) (2016) 9-13.

[13] D. Hiller et al., "Low temperature silicon dioxide by thermal atomic layer deposition: investigation of material properties", J. Appl. Phys., 107 (2010) 064314-1–064314-10.

[14] Y. Inoue and O. Takai, "Spectroscopic studies on preparation of silicon oxide films by PECVD using organosilicon compounds", Plasma Sources Sci. Technol., 5 (1996) 339-343.

[15] O.A. Hammadi, "Photovoltaic properties of thermally-grown selenium-doped silicon photodiodes for infrared detection applications," Phot. Sens., 5(2) (2015) 152–158.

[16] S. Kamiyama, T. Miura and Y. Nara, "Comparison between SiO_2 films deposited by atomic layer deposition with $SiH_2[N(CH_3)_2]_2$ and $SiH[N(CH_3)_2]_3$ precursors", Thin Solid Films, 515 (2006) 1517-1521.

[17] J.W. Klaus et al., "Atomic layer controlled growth of SiO_2 films using binary reaction sequence chemistry", Appl. Phys. Lett., 70 (1997) 1092–1094.

[18] J.-H. Lee et al., "Investigation of silicon oxide thin films prepared by atomic layer deposition using SiH_2Cl_2 and O_3 as the precursors", Jpn. J. Appl. Phys., 43 (2004) L328–L330.

[19] O.A. Hamadi, "Effect of annealing on the electrical characteristics of CdO-Si heterostructure produced by plasma-induced bonding technique," Iraqi J. Appl. Phys., 4(3) (2008) 34–37.

[20] O.A. Hammadi, M.K. Khalaf and F.J. Kadhim, "Fabrication and characterization of UV photodetectors based on silicon nitride nanostructures prepared by magnetron sputtering," Proc. IMechE Part N: J. Nanoeng. Nanosys., 230(1) (2015) 32–36.

[21] O.A. Hammadi, M.K. Khalaf and F.J. Kadhim, "Fabrication of UV photodetector from nickel oxide nanoparticles deposited on silicon substrate by closed-field unbalanced dual magnetron sputtering techniques," Opt. Quantum Electron., 47(2) (2015) 1–9.

[22] P. Pan, "The composition and properties of PECVD silicon oxide films", J. Electrochem. Soc., 132 (1985) 2012–2019.

